Quantum critical point in high-temperature superconductors

V.R. Shaginyan,[1,2,*] M.Ya. Amusia,[2] K.G. Popov,[3] and V.A. Stephanovich[4]

[1] *Petersburg Nuclear Physics Institute, RAS, Gatchina, 188300, Russia*
[2] *Racah Institute of Physics, Hebrew University, Jerusalem 91904, Israel*
[3] *Komi Science Center, Ural Division, RAS, Syktyvkar, 167982, Russia*
[4] *Opole University, Institute of Mathematics and Informatics, Opole, 45-052,Poland*[†]

Recently, in high-T_c superconductors (HTSC), exciting measurements have been performed revealing their physics in superconducting and pseudogap states and in normal one induced by the application of magnetic field, when the transition from non-Fermi liquid to Landau Fermi liquid behavior occurs. We employ a theory, based on fermion condensation quantum phase transition which is able to explain facts obtained in the measurements. We also show, that in spite of very different microscopic nature of HTSC, heavy-fermion metals and 2D ^{3}He, the physical properties of these three classes of substances are similar to each other.

PACS numbers: 72.15.Qm, 71.27.+a, 74.20.Fg, 74.25.Jb
Keywords: Quantum criticality; Heavy-fermion metals; High-temperature superconductivity

INTRODUCTION

Non-Fermi liquid (NFL) behavior of many classes of strongly correlated fermion systems projects one of the tremendous challenges in modern condensed matter physics. This behavior is so unusual that the traditional Landau paradigm of quasiparticles does not apply to it. It is widely believed that utterly new concepts are required to describe the underlying physics [1, 2, 3, 4, 5, 6]. There is a fundamental question: how many concepts do we need to describe the above physical mechanisms? This cannot be answered on purely experimental or theoretical grounds. Rather, we have to use both of them. Recently, in high-T_c superconductors (HTSC), exciting measurements revealing their physics have been performed. One type of the measurements demonstrate the existence of Bogoliubov quasiparticles (BQ) in a superconducting state [7, 8, 9]. At the same time, in the pseudogap regime at $T > T_c$ (when the superconductivity vanishes), a strong indication of the pairing of electrons or the formation of preformed electron pairs has been observed, while the gap continues to follow a simple d-wave form [8, 9]. Another type of the measurements explore the normal state induced by the application of magnetic field, when transition from NFL to Landau Fermi liquid (LFL) behavior occurs [10]. This transition takes place at magnetic field $B \geq B_{c2} \geq B_{c0}$, where B_{c2} is the field destroying the superconducting state, and B_{c0} is the critical field at which the magnetic field induced quantum critical point (QCP) takes place [10]. We note that to study the aforementioned transition experimentally, the strong magnetic fields $B \geq B_{c2}$ are required so that earlier such investigation was technically inaccessible. An attempt to study the transition experimentally had been done more than 10 years ago [11].

Many puzzling and common experimental features of such seemingly different systems as two-dimensional (2D) electron systems and liquid ^{3}He, heavy-fermion (HF) metals and HTSC suggest that there is a hidden phase transition, which remains to be recognized. The key word here is quantum criticality, taking place at QCP. Heavy fermion metals provide important examples of strongly correlated Fermi-systems. The second class of substances to test whether or not Landau quasiparticles [12] play an underlying role to construct the superconducting state and to form BQ on their base in accordance with Bardeen-Cooper-Schrieffer (BCS) theory [13], are HTSC. In these substances, all QCP are almost inaccessible to experimental observations since they are "covered" by superconductivity. More precisely, the superconductive gap opened at the Fermi level, changes the physical properties of corresponding quantum phase transition.

There is a common wisdom that the physical properties of above systems are related to zero temperature quantum fluctuations, suppressing quasiparticles and thus generating their NFL properties [1, 2, 3, 4, 5, 6], depending on their ground state, either magnetic or superconductive. On the other hand, it was shown that the electronic system of HF metals demonstrates the universal low-temperature behavior irrespectively of their magnetic ground state [14]. Recently, the NFL behavior has been discovered experimentally in 2D ^{3}He [15], and the theoretical explanation has been given to it [16], revealing the similarity in physical properties of 2D ^{3}He and HF metals. We note here that ^{3}He consists of neutral atoms interacting via van der Waals forces, while the mass of He atom is 3 orders of magnitude larger than that of an electron, making ^{3}He to have drastically different microscopic properties than those of HF metals. Therefore it is of crucial importance to check whether this behavior can be observed in other Fermi systems like HTSC. As we shall see, the precise measurements on HTSC's $Bi_2Sr_2Ca_2Cu_3O_{10+x}$ [7], $Bi_2Sr_2CaCu_2O_{8+x}$ [9] and $Tl_2Ba_2CuO_{6+x}$ [10] allow us to establish the relationships between physical properties of both HTSC

compounds and HF metals and clarify the role of Landau quasiparticles.

In this letter, we consider a superconducting state of HTSC in the framework of our theory based on the fermion condensation quantum phase transition (FCQPT) concept. We show that the superconducting state is BCS-like, the elementary excitations are BQ, and the primary ideas of the LFL and BCS theories remain valid, whereas the maximal value of a superconducting gap and other exotic properties are determined by the presence of underlying fermion condensate (FC). This presence manifests itself in a fact that the quasiparticle effective mass M^* strongly depends on temperature, magnetic field and doping x. We show, that in spite of very different microscopic nature of HTSC, HF metals and 2D ^{3}He, their physical properties belong to universal behavior of strongly correlated Fermi-systems. We demonstrate that the physics underlying the field-induced reentrance of LFL behavior is the same for HTSC compounds and HF metals. We demonstrate that there is at least one quantum phase transition inside the superconducting dome, and this transition is indeed FCQPT. We also show that there is a relationship between the critical fields B_{c2} and B_{c0} so that $B_{c2} \gtrsim B_{c0}$.

SUPERCONDUCTING AND PSEUDOGAP STATES

At $T < T_c$, the thermodynamic potential Ω of an electron liquid is given the equation (see, e.g. [22])

$$\Omega = E_{\rm gs} - \mu N - TS, \tag{1}$$

where N is particles number, S denotes the entropy, and μ is a chemical potential. The ground state energy $E_{\rm gs}[\kappa(\mathbf{p}), n(\mathbf{p})]$ of an electron liquid is a functional of superconducting order parameter $\kappa(\mathbf{p})$ and of the quasiparticle occupation numbers $n(\mathbf{p})$. Here we assume that the electron system is two-dimensional, while all results can be easily generalized to the case of three-dimensional system. The energy $E_{\rm gs}$ is determined by the standard equation of the weak-coupling theory of superconductivity

$$E_{\rm gs} = E[n(\mathbf{p})] + \int \lambda_0 V(\mathbf{p}_1, \mathbf{p}_2)\kappa(\mathbf{p}_1)\kappa^*(\mathbf{p}_2)\frac{d\mathbf{p}_1 d\mathbf{p}_2}{(2\pi)^4}. \tag{2}$$

Here $E[n(\mathbf{p})]$ is the Landau functional determining the ground-state energy of a normal Fermi liquid. Here $\lambda_0 V$ is the pairing interaction and λ_0 is the coupling constant. Here

$$n(\mathbf{p}) = v^2(\mathbf{p})\left[1 - f(\mathbf{p})\right] + u^2(\mathbf{p})f(\mathbf{p}), \tag{3}$$

and

$$\kappa(\mathbf{p}) = v(\mathbf{p})u(\mathbf{p})\left[1 - 2f(\mathbf{p})\right], \tag{4}$$

where the coherence factors $v(\mathbf{p})$ and $u(\mathbf{p})$ are obeyed the normalization condition

$$v^2(\mathbf{p}) + u^2(\mathbf{p}) = 1. \tag{5}$$

The distribution function $f(\mathbf{p})$ of BQ defines the entropy

$$S = -2\int \left[f(\mathbf{p})\ln f(\mathbf{p}) + (1 - f(\mathbf{p}))\ln(1 - f(\mathbf{p}))\right]\frac{d\mathbf{p}}{4\pi^2}. \tag{6}$$

We assume that the pairing interaction $\lambda_0 V$ is weak and produced, for instance, by electron-phonon interaction. Minimizing Ω with respect to $\kappa(\mathbf{p})$ and using the definition $\Delta(\mathbf{p}) = -\delta\Omega/\kappa(\mathbf{p})$, we obtain

$$\Delta(\mathbf{p}) = -\int \lambda_0 V(\mathbf{p}, \mathbf{p}_1)\kappa(\mathbf{p}_1)\frac{d\mathbf{p}_1}{(2\pi)^2}, \tag{7}$$

$$\varepsilon(\mathbf{p}) - \mu = \Delta(\mathbf{p})\frac{1 - 2v^2(\mathbf{p})}{2v(\mathbf{p})u(\mathbf{p})}. \tag{8}$$

The single-particle energy $\varepsilon(\mathbf{p})$ is determined by the Landau equation

$$\varepsilon(\mathbf{p}) = \frac{\delta E[n(\mathbf{p})]}{\delta n(\mathbf{p})}. \tag{9}$$

Note that $E[n(\mathbf{p})]$, $\varepsilon[n(\mathbf{p})]$, and the Landau amplitude

$$F_L(\mathbf{p}, \mathbf{p}_1) = \frac{\delta^2 E[n(\mathbf{p})]}{\delta n(\mathbf{p})\delta n(\mathbf{p}_1)} \tag{10}$$

depend implicitly on the density x which defines the strength of F_L. Minimizing Ω with respect to $f(\mathbf{p})$ and after some algebra, we obtain the following explicit equation for the superconducting gap $\Delta(\mathbf{p})$

$$\Delta(\mathbf{p}) = -\frac{1}{2}\int \lambda_0 V(\mathbf{p}, \mathbf{p}_1)\frac{\Delta(\mathbf{p}_1)}{E(\mathbf{p}_1)}\left[1 - 2f(\mathbf{p}_1)\right])\frac{d\mathbf{p}_1}{4\pi^2}. \tag{11}$$

Here the excitation energy $E(\mathbf{p})$ of BQ is given by

$$E(\mathbf{p}) = \frac{\delta(E_{gs} - \mu N)}{\delta f(\mathbf{p})} = \sqrt{(\varepsilon(\mathbf{p}) - \mu)^2 + \Delta^2(\mathbf{p})}. \tag{12}$$

The coherence factors $v(\mathbf{p})$, $u(\mathbf{p})$, and the distribution function $f(\mathbf{p})$ are given by the ordinary relations

$$v^2(\mathbf{p}) = \frac{1}{2}\left[1 - \xi(\mathbf{p})\right], \quad u^2(\mathbf{p}) = \frac{1}{2}\left[1 + \xi(\mathbf{p})\right], \tag{13}$$

$$\xi(\mathbf{p}) = \frac{\varepsilon(\mathbf{p}) - \mu}{E(\mathbf{p})}, \quad f(\mathbf{p}) = \frac{1}{1 + \exp(E(\mathbf{p})/T)}. \tag{14}$$

The equations (8)-(14) are conventional BSC equations [13, 22] for the superconducting state with BQ and the maximal value of the superconducting gap $\Delta_1 \propto \exp(-1/\lambda_0)$ if the system in question has not undergone FCQPT.

Now we consider a superconducting electron liquid with FC taking place after FCQPT point. If $T = 0$ and $\lambda_0 \to 0$, then both maximal value of the superconducting gap $\Delta_1 \to 0$ and the critical temperature $T_c \to 0$ so that Eq. (8) reduces to the equation [17, 18, 19, 20, 21, 23, 24]

$$\frac{\delta E}{\delta n(\mathbf{p})} = \varepsilon(\mathbf{p}) = \mu, \text{ if } 0 \le n(\mathbf{p}) \le 1;\ p_i \le p \le p_f \quad (15)$$

provided that the order parameter κ is finite at $p_i \le p \le p_f$. Equation (15) defines a new state of electron liquid with FC characterized by a flat part of the spectrum in the $p_f - p_i$ region. This state has a strong impact on the system properties and emerges at some critical density $x = x_{FC}$ where the amplitude F_L becomes strong enough. On the contrary, when the Landau amplitude $F_L(p = p_F, p_1 = p_F)$ as a function of density x is sufficiently small, the flat part vanishes, and at $T \to 0$ Eq. (15) has the only trivial solution $\varepsilon(p = p_F) = \mu$ so that the quasiparticle occupation numbers are given by a step function, $n(\mathbf{p}) = \theta(p_F - p)$.

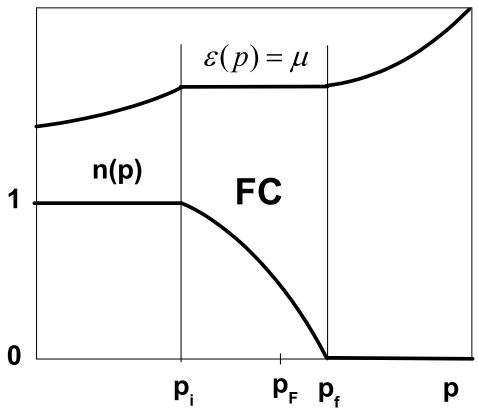

FIG. 1: Schematic plot of the quasiparticle occupation number $n(p)$ and spectrum $\varepsilon(p)$ in the FC state. Function $n(p)$ obeys the relations $n(p \le p_i) = 1$, $n(p_i < p < p_f) < 1$ and $n(p \ge p_f) = 0$, while $\varepsilon(p_i < p < p_f) = \mu$. Fermi momentum p_F satisfies the condition $p_i < p_F < p_f$.

Upon applying well-known Landau equation, we can relate a quasiparticle effective mass M^* to the bare electron mass M [12, 25]

$$\frac{M^*}{M} = \frac{1}{1 - N_0 F^1(x)/3}. \quad (16)$$

Here N_0 is the density of states of a free electron gas, $x = p_F^3/3\pi^2$ is a number density, p_F is Fermi momentum, and $F^1(x)$ is the p-wave component of Landau interaction F_L. When at critical density $x = x_{FC}$, $F^1(x)$ achieves a threshold value, the denominator in Eq. (16) tends to zero so that the effective mass diverges at $T = 0$ and the system undergoes FCQPT. The leading term of this divergence reads

$$\frac{M^*(x)}{M} = \alpha_1 + \frac{\alpha_2}{x - x_{FC}}, \quad (17)$$

where α_1 and α_2 are constants. At $x < x_{FC}$ the FC takes place. The essence of this phenomenon is that at $x < x_c$ the effective mass (17) becomes negative signifying physically meaningless state. To avoid this state, the system reconstructs its quasiparticle occupation number $n(\mathbf{p})$ and topological structure so as to minimize its ground state energy E. The main result of such reconstruction is that instead of Fermi step, we have $0 \le n(p) \le 1$ in certain range of momenta $p_i \le p \le p_f$, see Eq. (15). Accordingly, in the above momenta interval, the spectrum $\varepsilon(p) = \mu$, see Fig. 1 for details of its modification.

Due to above peculiarities of the $n(\mathbf{p})$ function, FC state is characterized by the superconducting order parameter $\kappa(\mathbf{p}) = \sqrt{n(\mathbf{p})(1 - n(\mathbf{p}))}$. This means that if the electron system with FC has pairing interaction with coupling constant λ, it exhibits superconductivity since as it follows from Eq. (7) $\Delta_1 \propto \lambda$ in a weak coupling limit. This linear dependence is also a peculiarity of FC state [17, 18, 20, 23] and substitutes above well-known BCS relation $\Delta_1 \propto \exp(-1/\lambda_0)$.

Now we can study the relation between the state defined by Eq. (15) and the superconductivity. At $T \to 0$, Eq. (15) defines a particular state of a Fermi liquid with FC, for which the modulus of the order parameter $|\kappa(\mathbf{p})|$ has finite values in the $(p_f - p_i)$ region, whereas $\Delta_1 \to 0$ in this region. We observe that $f(\mathbf{p}, T \to 0) \to 0$, and it follows from Eqs. (3) and (4) that $0 < n(\mathbf{p}) < 1$ implies that $|\kappa(\mathbf{p})| \ne 0$ in the region $(p_f - p_i)$. Such a state can be considered as superconducting with an infinitely small value of Δ_1 so that the entropy of this state is equal to zero. It is obvious that this state being driven by the quantum phase transition disappears at $T > 0$ [23]. Any quantum phase transition at $T = 0$ is determined by a control parameter other then temperature, for example, by pressure, by magnetic field, or by the density x of mobile charge carriers. Since a quantum phase transition occurs at a QCP, in our FCQPT case at $T = 0$ the role of QCP is played by critical density $x = x_{FC}$.

If $\lambda_0 \ne 0$, then Δ_1 becomes finite. It is seen from Eq. (11) that the superconducting gap depends on the single-particle spectrum $\varepsilon(\mathbf{p})$. On the other hand, it follows from Eq. (8) that $\varepsilon(\mathbf{p})$ depends on $\Delta(\mathbf{p})$ provided that at $\Delta_1 \to 0$ Eq. (15) has the solution corresponding to FC existence. Let us assume that λ_0 is small so that the BSC interaction $\lambda_0 V(\mathbf{p}, \mathbf{p}_1)$ can only lead to a small correction to the order parameter $\kappa(\mathbf{p})$ determined by Eq. (15). Upon differentiation both parts of Eq. (8)

over momentum p, we obtain that M^* becomes finite

$$M^* \sim p_F \frac{p_f - p_i}{2\Delta_1}. \tag{18}$$

It follows from Eq. (18) that the effective mass and the density of states $N(0) \propto M^* \propto 1/\Delta_1$ are finite and constant at $T < T_c$. As a result, we conclude that in contrast to the conventional theory of superconductivity the single-particle spectrum $\varepsilon(\mathbf{p})$ strongly depends on the superconducting gap and we have to solve Eqs. (9) and (11) self-consistently. On the other hand, let us assume that Eqs. (9) and (11) are solved, and the effective mass M^* is determined. Now one can fix the dispersion $\varepsilon(\mathbf{p})$ by choosing the effective mass M^* of system in question equal to M^*_{FC} and then solve Eq. (11) as it is done in the case of the conventional theory of superconductivity [13]. As a result, one observes that the superconducting state is characterized by BQ with the dispersion (12), the coherence factors u, v (13) and normalization condition (5). Thus, the observed features agree with BQ behavior predicted by BCS theory. This suggests that at $T \leq T_c$ the superconducting state with FC is BCS-like and implies the basic validity of BCS formalism for the description of this state. It is exactly the case observed experimentally in HTSC's $Bi_2Sr_2Ca_2Cu_3O_{10+x}$ and $Bi_2Sr_2CaCu_2O_{8+x}$ [7, 9].

It has been shown in Refs [20, 26], that in the presence of FC, Eq. (11) has nontrivial solutions at $T < T^*$ (T^* is a temperature at which Eq. (11) has only trivial solution $\Delta = 0$) when the pairing interaction $\lambda_0 V$ consists of attraction and strong repulsion leading to d-wave superconductivity. At some temperature $T_{\rm node}$, the gap $\Delta(\mathbf{p})$ as a function of the angle ϕ ($\Delta(\mathbf{p}) = \Delta(p_F, \phi)$) obtains new nodes as shown in Fig. 2 [26]. Figure 2 shows the ratio $\Delta(p_F, \phi)/T^*$ calculated for three temperatures: $0.9\,T_{\rm node}$, $T_{\rm node}$ and $1.2\,T_{\rm node}$. In contrast to curve (a), curves (b) and (c) have approximately flat sections. Clearly, the flattening occurs due to new zeros emerging at $T = T_{\rm node}$, see Fig. 2. As the temperature increases, the region θ_c between zeros (indicated by arrows in Fig. 2) increases in size. It is also clear that the gap Δ is very small within the interval θ_c. Thus, we conclude that the gap in the vicinity of θ_c can be destroyed at $T \geq T_c$ by any strong fluctuations (e.g. antiferromagnetic), impurities, and sizable inhomogeneities existing in HTSC. Since the superconducting gap is destroyed in a macroscopic region of the phase space, θ_c, the coherence necessary for superconductivity is vanished and superconductivity is also destroyed. This observation allows us to conclude that $T_c \simeq T_{\rm node}$, while at $T \geq T_c$ the pseudogap is formed. The behavior and the shape of the pseudogap resembles closely similar characteristics of the superconducting gap as Fig. 2 shows. The main difference is that the pseudogap disappears in the segment θ_c of the Fermi surface, while the gap disappears at isolated nodes of the d-wave. Our estimates

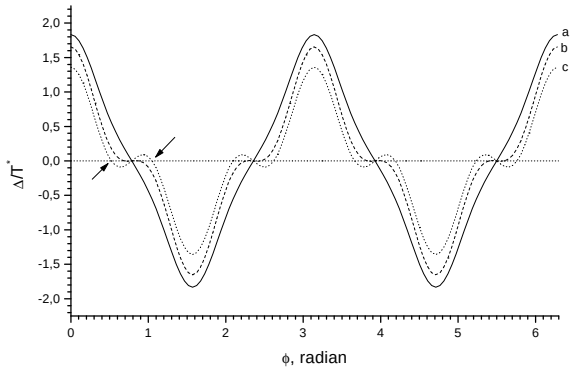

FIG. 2: The gap $\Delta(p_F, \phi)$ as a function of ϕ calculated for three values of the temperature T in units of $T_{\rm node} \simeq T_c$. The curve (a) (solid line) represents the calculation for $T = 0.9T_{\rm node}$, the curve (b) (dashed line) represents the same at $T = T_{\rm node}$ and the curve (c) (dotted line) reports the calculation at $T = 1.2T_{\rm node}$. The arrows indicate the region θ_c limited by the two new zeros emerging at $T > T_{\rm node}$.

show that for small values of the angle ψ, the function $\theta_c(\psi)$ rapidly increases, $\theta_c(\psi) \simeq \sqrt{\psi}$. These estimates agree with the results of numerical calculations of the function $\theta_c([T - T_c]/T_c)$.

At temperatures $T < T_c$, the quasiparticle excitations of the superconducting state are characterized by the presence of sharp peaks. When the temperature becomes high ($T > T_c$) and $\Delta(\theta) \equiv 0$ in the interval θ_c, normal quasiparticle excitations with a width γ appear in the segments θ_c of the Fermi surface. A pseudogap exists outside the segments θ_c, and the Fermi surface is occupied by BQ in this region. Excitations of both types have widths of the same order of magnitude, transferring their energy and momenta into excitations of normal quasiparticles. We estimate the value of γ. If the entire Fermi surface were occupied by the normal state, the width γ would be $\gamma \approx N(0)^3 T^2/\epsilon(T)^2$ with the density of states $N(0) \sim M^*(T) \sim 1/T$. The dielectric constant $\epsilon(T) \sim N(0)$ and hence $\gamma \sim T$ [18]. However, only a part of the Fermi surface within θ_c is occupied by normal excitations in our case. Therefore, the number of states accessible for quasiparticles and quasiholes is proportional to θ_c, and the factor T^2 is replaced by the factor $T^2\theta_c^2$. Taking all this into account yields $\gamma \sim \theta_c^2 T \sim T(T - T_c)/T_c \sim (T - T_c)$. Here, we ignored the small contribution from BCS - type excitations. It is precisely for this reason that the width γ vanishes at $T = T_c$, while the resistivity of the normal state $\rho(T) \propto \gamma \propto (T - T_c)$, because $\gamma \sim T - T_c$.

GENERAL PROPERTIES OF HEAVY-FERMION METALS

We have shown earlier (see, e.g. [20]) that without loss of generality, to study the above universal behavior, it is sufficient to use the simplest possible model of a homogeneous heavy-electron (fermion) liquid. This permits not only to better reveal the physical nature of observed effects, but to avoid unnecessary complications related to microscopic features (like crystalline structure, defects and impurities etc) of specific substances.

Now we consider the action of external magnetic field on HF liquid in FC phase. Assume now that λ_0 is infinitely small. Any infinitesimal magnetic field $B \neq 0$ (better to say, $B \geq B_{c0}$) destroys both superconductivity and FC state, splitting it by Landau levels. The simple qualitative arguments can be used to guess what happens to FC state in this case. On one side, the energy gain from FC state destruction is $\Delta E_B \propto B^2$ (see above) and tends to zero as $B \to 0$. On the other side, $n(p)$ in the interval $p_i \leq p \leq p_f$ gives a finite energy gain as compared to the ground state energy of a normal Fermi liquid [20]. It turns out that the state with largest possible energy gain is formed by a multiconnected Fermi surface, so that the smooth function $n(p)$ is replaced in the interval $p_i \leq p \leq p_f$ by the set of rectangular blocks of unit height, formed from Heavyside step functions [21, 27, 28]. In this state the system demonstrates LFL behavior, while the effective mass strongly depends on magnetic field [20, 28],

$$M^*(B) \propto \frac{1}{\sqrt{B - B_{c0}}}. \tag{19}$$

Here B_{c0} is the critical magnetic field driving corresponding QCP towards $T = 0$. In some cases, for example in HF metal $CeRu_2Si_2$, $B_{c0} = 0$, see e.g. [29]. In our simple model B_{c0} is taken as a parameter.

At elevated temperatures, the system transits from the LFL to NFL regime as shown by the solid vertical arrow in Fig. 3 exhibiting the low-temperature universal behavior independent of its magnetic ground state, composition, dimensionality (2D or 3D) and even nature of constituent Fermi particles which may be electrons or ^{3}He atoms [14, 16]. To check, whether the quasiparticles are present in the systems in the transition regime, we use the results of measurements of heat capacity C, entropy S and magnetic susceptibility χ. If these results can be fitted by the well-known relations from Fermi liquid theory $C/T = \gamma_0 \propto S/T \propto \chi \propto M^*$, then quasiparticles define the system properties in the transition regime.

Consider temperature and magnetic field dependence of the effective mass $M^*(T, B)$ as system approaches FCQPT. Landau equation [12] is of the form

$$\frac{1}{M^*} = \frac{1}{M} + \int \frac{\mathbf{p}_F \mathbf{p}_1}{p_F^3} F_L(\mathbf{p_F}, \mathbf{p}_1) \frac{\partial n(p_1, T, B)}{\partial p_1} \frac{d\mathbf{p}_1}{(2\pi)^3}. \tag{20}$$

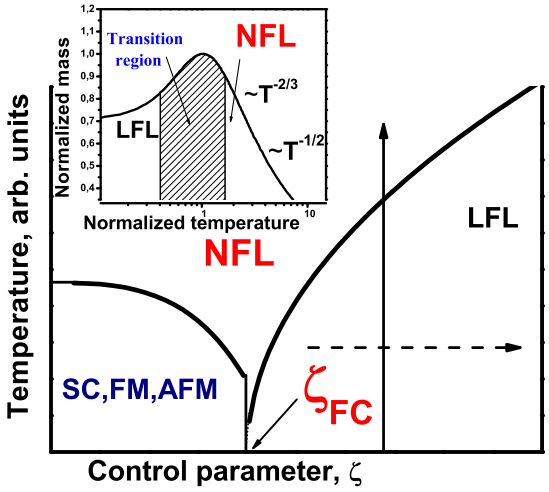

FIG. 3: Schematic phase diagram of HF metal. Control parameter ζ represents doping x, magnetic field B, pressure P etc. $\zeta_{\rm FC}$ denotes the point of effective mass divergence. The vertical arrow shows LFL-NFL transitions at fixed ζ with M^* depending on T_N as given by Eq. (21). The dash horizontal arrow illustrates the system moving in LFL regime along ζ at fixed T_N, while $M^*(B)$ is given by Eq. (19). At $\zeta < \zeta_{\rm FC}$ the system can be in a superconducting (SC), ferromagnetic (FM) or antiferromagnetic (AFM) states. Inset shows a schematic plot of the normalized effective mass versus the normalized temperature. Transition regime, where M_N^* reaches its maximum, is shown by the hatched area.

Here we suppress the spin indices for simplicity. When the system is near FCQPT, the approximate interpolative solution for Eq. (20) reads [14, 16, 20]

$$\frac{M^*(T_N, x)}{M_M^*} = M_N^*(T_N) \approx c_0 \frac{1 + c_1 T_N^2}{1 + c_2 T_N^{8/3}}. \tag{21}$$

Here $M_N^*(T_N)$ is the normalized effective mass, M_M^* is the maximum value, that it reaches at $T = T_M$. Normalized temperature $T_N = T/T_M$, $c_0 = (1+c_2)/(1+c_1)$, c_1 and c_2 are fitting parameters, parameterizing Landau amplitude. It follows from Eq. (21) that in contrast to the standard paradigm of quasiparticles the effective mass strongly depends on temperature, revealing three different regimes at growing temperature. At the lowest temperatures we have the LFL regime. Then the system enters the transition regime: $M_N^*(T_N)$ grows, reaching its maximum $M_N^* = 1$ at $T = T_M$, $(T_N = 1)$, with subsequent diminishing. Near temperatures $T_N \geq 1$ the last "traces" of LFL regime disappear and the NFL state takes place, manifesting itself in decreasing of M_N^* as $T_N^{-2/3}$ and then as

$$M_N^*(T_N) \propto \frac{1}{\sqrt{T_N}}. \tag{22}$$

These regimes are reported in the inset to Fig. 3.

As it follows from Eq. (21), M^* reaches the maximum M^*_M at some temperature T_M. Since there is no external physical scales near FCQPT point, the normalization of both M^* and T by internal parameters M^*_M and T_M immediately reveals the common physical nature of above thermodynamic functions which we use to extract the effective mass. The normalized effective mass extracted from measurements on the HF metals $YbRh_2(Si_{0.95}Ge_{0.05})_2$ [30, 31], $CeRu_2Si_2$ [29], $CePd_{1-x}Rh_x$ [32], and 2D ^{3}He [15] along with our theoretical solid curve (also shown in the inset) is reported in Fig. 4. It is seen that above normalization of experimental data yields the merging of multiple curves into single one, thus demonstrating a universal scaling behavior [14, 16, 33]. It is also seen that the universal behavior of the effective mass given by our theoretical curve agrees well with experimental data.

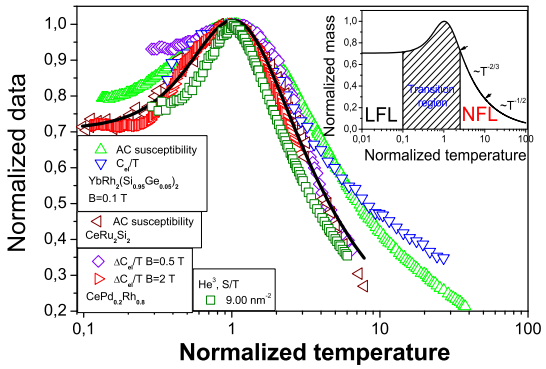

FIG. 4: The universal behavior of $M^*_N(T_N)$, extracted from measurements of different thermodynamic quantities, as shown in the legend. The AC susceptibility, $\chi_{AC}(T,B)$, is taken for $YbRh_2(Si_{0.95}Ge_{0.05})_2$ and $CeRu_2Si_2$ [29, 30], the heat capacity divided by temperature, C/T, is taken for $YbRh_2(Si_{0.95}Ge_{0.05})_2$ and $CePd_{0.2}Rh_{0.8}$ [31, 32] and entropy divided by temperature, S/T, for 2D ^{3}He is taken from Ref. [15]. The solid curve gives the theoretical universal behavior of M^*_N determined by Eq. (21). Inset shows normalized effective mass $M^*_N(T_N)$ (21) versus the normalized temperature $T_N = T/T_M$. The hatched area outlines the transition regime. Several regions are shown as explained in the text.

It is seen from Fig. 4 that at $T/T_M = T_N \leq 1$ the T-dependence of the effective mass is weak. This means that the T_M point can be regarded as a crossover between LFL and NFL regimes. Since magnetic field enters the Landau equation as $\mu_B B/T$, we have

$$T^*(B) = a_1 + a_2 B \simeq T_M \sim \mu_B(B - B_{c0}), \qquad (23)$$

where $T^*(B)$ is the crossover temperature, μ_B is Bohr magneton, a_1 and a_2 are constants. The crossover temperature is not really a phase transition. It necessarily is broad, very much depending on the criteria for determination of the point of such a crossover, as it is seen from the inset to Fig. 4. As usually, the temperature $T^*(B)$ is extracted from the field dependence of charge transport, for example from the resistivity $\rho(T) = \rho_0 + A(B)T^2$ with ρ_0 is a temperature independent part and $A(B)$ is a LFL coefficient. The crossover takes place at temperatures where the resistance starts to deviate from the LFL T^2 behavior, see e.g. Ref. [10]. We note that Eq. (19) is valid at $T < T^*(B)$. In that case, magnetic field plays a role of the control parameter ζ at fixed T_N as shown in Fig. 3 by the dash horizontal arrow.

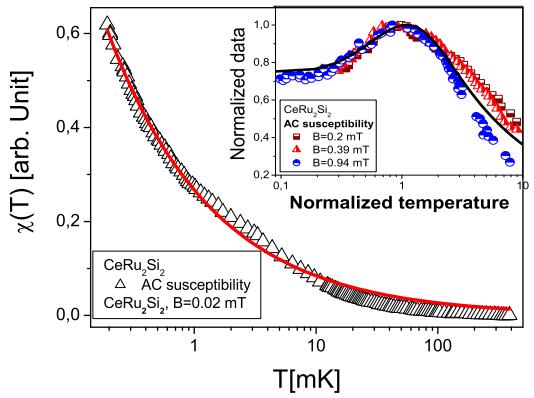

FIG. 5: Temperature dependence of the AC susceptibility χ_{AC} for $CeRu_2Si_2$. The solid curve is a fit for the data shown by the triangles at $B = 0.02$ mT [29] and represented by the function $\chi(T) = a/\sqrt{T}$ given by Eq. (22) with a being a fitting parameter. Inset reports $M^*_N(T_N)$ extracted from χ_{AC} measured at different fields as indicated in the legend [29]. The solid curve traces the universal behavior (21). Parameters c_1 and c_2 are adjusted to fit the average behavior of the normalized effective mass M^*_N.

To verify Eq. (22) and illustrate the transition from LFL to NFL regime, we use measurements of $\chi_{AC}(T)$ in $CeRu_2Si_2$ at magnetic field $B = 0.02$ mT at which this HF metal demonstrates the NFL behavior down to lowest temperatures [29]. Indeed, in this case we expect that LFL regime emerges at temperatures lower than $T_M \sim \mu_B B \sim 0.01$ mK as it follows from Eq. (23). It is seen from Fig. 5 that Eq. (22) gives good description of the facts in the extremely wide temperature range: the susceptibility χ_{AC} as a function of T, is not a constant upon cooling, as would be for a Fermi liquid, but shows a $1/\sqrt{T}$ divergence over more than three decades in temperature. The inset to Fig. 5 exhibits a fit for M^*_N extracted from measurements of $\chi_{AC}(T)$ at different magnetic fields, clearly indicating the transition from LFL behavior at $T_N < 1$ to NFL one at $T_N > 1$ when the system moves along the vertical arrow in Fig. 3. It

seen from Fig. 5 that the function given by Eq. (21) represents a good approximation for M_N^*.

COMMON FIELD-INDUCED QUANTUM CRITICAL POINT IN HTSC COMPOUNDS AND HF METALS

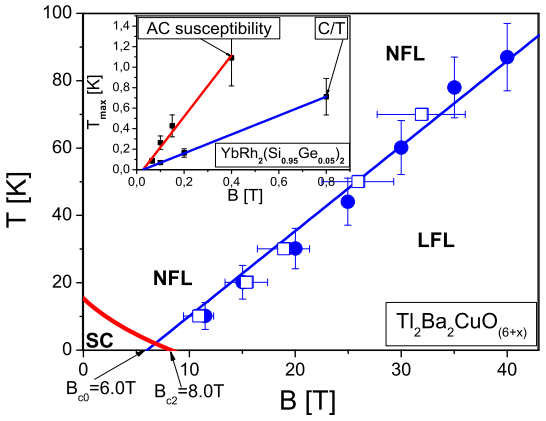

FIG. 6: $B-T$ phase diagram of superconductor $Tl_2Ba_2CuO_{6+x}$. The crossover (from LFL to NFL regime) line $T^*(B)$ is given by the Eq. (23). Open squares and solid circles are experimental values [10]. Thick line represents the boundary between the superconducting and normal phases. Arrows near the bottom left corner indicate the critical magnetic field B_{c2} destroying the superconductivity and the critical field B_{c0}. Inset reports the peak temperatures $T_{\max}(B)$, extracted from measurements of C/T and χ_{AC} on $YbRh_2(Si_{0.95}Ge_{0.05})_2$ [30, 31] and approximated by straight lines (23). The lines intersect at $B \simeq 0.03$ T.

Let us now consider the $B-T$ phase diagram of the HTSC substance $Tl_2Ba_2CuO_{6+x}$ shown in Fig. 6. The substance is a superconductor with T_c from 15 K to 93 K depending on oxygen content [10]. In Fig. 6, open squares and solid circles show the experimental values of the crossover temperature from the LFL to NFL regimes [10]. The solid line shows our fit (23) with $B_{c0} = 6$ T that is in good agreement with $B_{c0} = 5.8$ T obtained from the field dependence of the charge transport [10]. As it is seen from Fig. 6, the linear behavior agrees well with experimental data [10]. The peak temperatures $T_{\max}$ shown in the inset to Fig. 6, report the maxima of $C(T)/T$ and $\chi_{AC}(T)$ measured on $YbRh_2(Si_{0.95}Ge_{0.05})_2$ [30, 31]. As it follows from Eq. (23), $T_{\max}$ shifts to higher values with increase of the applied magnetic field. It is seen that both functions can be represented by straight lines intersecting at $B \simeq 0.03$ T. This observation is in good agreement with experiments [30, 31]. It is seen from Fig. 6 that critical field $B_{c2} = 8$ T destroying the superconductivity is close to $B_{c0} = 6$ T. Let us show that this

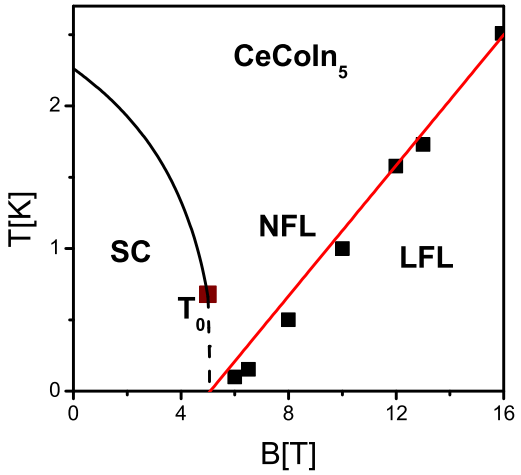

FIG. 7: $B-T$ phase diagram of the $CeCoIn_5$ heavy fermion metal. The crossover line between superconducting and normal phases is shown by the solid line at $T > T_0$ and dashed one at $T < T_0$. The point T_0, shown by square signifies a temperature, where the phase transition becomes a first-order (at $T < T_0$ [37]). The solid straight line specified by Eq. (23) with the experimental points [38] shown by squares is a boundary between Landau Fermi liquid (LFL) and non-Fermi-liquid (NFL) states.

is more than a simple coincidence, and $B_{c2} \gtrsim B_{c0}$. Indeed, at $B > B_{c0}$ and low temperatures $T < T^*(B)$, the system is in its LFL state. The superconductivity is then destroyed since the superconducting gap is exponentially small as we have seen above. At the same time, there is FC state at $B < B_{c0}$ and this low-field phase has large prerequisites towards superconductivity as in this case the gap is a linear function of the coupling constant as it was also shown above. We note that this is exactly the case in $CeCoIn_5$ where $B_{c0} \simeq B_{c2} \simeq 5$ T [34] as seen from Fig. 7, while the application of pressure makes $B_{c2} > B_{c0}$ [35]. On the other hand, if the superconducting coupling constant is rather weak then antiferromagnetic order wins a competition. As a result, $B_{c2} = 0$, while B_{c0} can be finite as in $YbRh_2Si_2$ and $YbRh_2(Si_{0.95}Ge_{0.05})_2$ [30, 36].

Upon comparing the phase diagrams of $Tl_2Ba_2CuO_{6+x}$ and $CeCoIn_5$ (Figs. 6 and 7 respectively), it is possible to conclude that they are similar in many respects. Further, we note that the superconducting boundary line $B_{c2}(T)$ at lowering temperatures acquires a step, i.e. the corresponding phase transition becomes first order [37, 39]. This permits us to speculate that the same may be true for $Tl_2Ba_2CuO_{6+x}$. We expect that in the NFL state the tunneling conductivity is asymmetric function of the applied voltage, while it becomes symmetric at the application of elevated magnetic fields when $Tl_2Ba_2CuO_{6+x}$ transits to the LFL regime, as it predicted to be in $CeCoIn_5$ [40].

Now we consider the field-induced reentrance of LFL

behavior in $Tl_2Ba_2CuO_{6+x}$ at $B \geq B_{c2}$. In that case, the effective mass M^* depends on magnetic field B taking the role of the control parameter ζ, while the system is in the LFL regime as it is shown by the dashed horizontal arrow in Fig. 3. The LFL regime is characterized by the temperature dependence of the resistivity, $\rho(T) = \rho_0 + A(B)T^2$, see also above. The A coefficient, being proportional to the quasiparticle–quasiparticle scattering cross-section, is found to be $A \propto (M^*(B))^2$ [36]. With respect to Eq. (19), this implies that

$$A(B) \simeq A_0 + \frac{D}{B - B_{c0}}, \qquad (24)$$

where A_0 and D are parameters. It is pertinent to note that Kadowaki-Woods ratio [41], $K = A/\gamma_0^2$, is constant within our FCQPT theory as it follows from Eqs. (19) and (24) [42]. It follows from Eq. (24) that it is impossible to observe the relatively high values of $A(B)$ since in our case $B_{c2} > B_{c0}$. We note that Eq. (24) is applicable when the superconductivity is destroyed by the application of magnetic field, otherwise the effective mass is also finite being given by Eq. (18). Therefore, as was mentioned above, in HTSC, a QCP is poorly accessible to experimental observations being *"hidden in superconductivity"*. Nonetheless, thanks to recent experimental facts [10], we will see that it is possible to study QCP by exploring its "shadows".

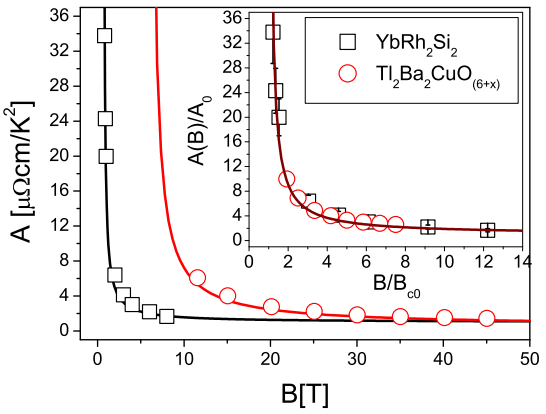

FIG. 8: The charge transport coefficient $A(B)$ as a function of magnetic field B obtained in measurements on $YbRh_2Si_2$ (squares) [36] and $Tl_2Ba_2CuO_{6+x}$ (circles) [10]. The different field scales are clearly seen. In the inset, normalized coefficient $A(B)/A_0 \simeq 1 + D_N/(y-1)$ as a function of normalized magnetic field $y = B/B_{c0}$ is shown by squares for $YbRh_2Si_2$ and by circles for $Tl_2Ba_2CuO_{6+x}$. D_N is the only fitting parameter.

Figure 8 reports the fit of our theoretical dependence (24) to the experimental data for two different classes of substances: HF metal $YbRh_2Si_2$ and HTSC $Tl_2Ba_2CuO_{6+x}$. The different scale of fields is clearly seen as well as good coincidence with theoretical dependence (24). This means that the physics underlying the field-induced reentrance of LFL behavior, is the same for both classes of substances. To further corroborate this point, we rewrite Eq. (24) in reduced variables A/A_0 and B/B_{c0}. Such rewriting immediately reveals the universal nature of the behavior of these two substances - both of them are driven to common QCP related to FC and induced by the application of magnetic field. As a result, Eq. (24) takes the form

$$\frac{A(B)}{A_0} \simeq 1 + \frac{D_N}{B/B_{c0} - 1}, \qquad (25)$$

where $D_N = D/(A_0 B_{c0})$ is a constant. It is seen from Eq. (25) that upon applying the scaling, the quantities $A(B)$ for $Tl_2Ba_2CuO_{6+x}$ and $YbRh_2Si_2$ are reduced to a function of the single variable B/B_{c0} thus demonstrating universal behavior. To support Eq. (25), we replot both dependencies in reduced variables A/A_0 and B/B_{c0} as it is depicted in the inset to Fig. 8. Such replotting immediately reveals the universal nature of the behavior of these two substances. It is seen from the inset to Fig. 8 that close to magnetic QCP there is no external physical scales so that the normalization by internal scales A_0 and B_{c0} shows straightforwardly the common physical nature of these substances behavior.

SUMMARY

Our comprehensive theoretical study of vast majority of experimental facts regarding very different strongly correlated Fermi-systems such as high-temperature superconductors, heavy-fermion compounds and two-dimensional ^{3}He clearly demonstrates their generic family resemblance. We show that the physics underlying the field-induced reentrance of LFL behavior is the same for both HTSC compounds and HF metals. We also show that there is a relationship between the critical fields B_{c2} and B_{c0} so that $B_{c2} \gtrsim B_{c0}$. It follows from our study that there is at least one quantum phase transition inside the superconducting dome, and this transition is the fermion condensation quantum phase transition.

This work was supported in part by the grants: RFBR No. 09-02-00056.

* Electronic address: vrshag@thd.pnpi.spb.ru
† Electronic address: stef@math.uni.opole.pl

[1] T. Senthil, M.P.A. Fisher, Phys. Rev. B 62 (2000) 7850.
[2] T. Senthil, M. Vojta, S. Sachdev, Phys. Rev. B 69 (2004) 035111.
[3] P. Coleman, A.J. Schofield, Nature 433 (2005) 226.

[4] H.v. Löhneysen, A. Rosch, M. Vojta, P. Wölfle, Rev. Mod. Phys. 79 (2007) 1015.
[5] P. Gegenwart, Q. Si, F. Steglich, Nature Phys., 4 (2008) 186.
[6] S. Sachdev, Nature Phys. 4 (2008) 173.
[7] H. Matsui, et al., Phys. Rev. Lett. 90 (2003) 217002.
[8] M. Shi, et al., Phys. Rev. Lett. 101 (2008) 047002.
[9] H.-B. Yang, et al., Nature 456 (2008) 77.
[10] T. Shibauchi, et al., Proc. Natl. Acad. Sci. USA 105 (2008) 7120.
[11] A.P. Mackenzie et. al., Phys. Rev. B 53 (1996) 5848.
[12] L. D. Landau, Sov. Phys. JETP 3 (1956) 920.
[13] J. Bardeen, L. Cooper, J.R. Shrieffer, Phys. Rev. 108 (1957) 1175.
[14] V.R. Shaginyan, K.G. Popov, V.A. Stephanovich, Europhys. Lett., 79 (2007) 47001.
[15] M. Neumann, J. Nyéki, J. Saunders, Science 317 (2007) 1356.
[16] V.R. Shaginyan, A.Z. Msezane, K.G. Popov, V.A. Stephanovich, Phys. Rev. Lett. 100 (2008) 096406.
[17] V.A. Khodel, V.R. Shaginyan, JETP Lett. 51 (1990) 553.
[18] V.A. Khodel, V.R. Shaginyan, V.V. Khodel, Phys. Rep. 249 (1994) 1.
[19] G.E. Volovik, *Quantum Phase Transitions from Topology in Momentum Space*, Lect. Notes in Physics, 718 (2007) 31.
[20] V.R. Shaginyan, M.Ya. Amusia, K.G. Popov, Physics-Uspekhi 50 (2007) 563.
[21] V.A. Khodel, J.W. Clark, and M.V. Zverev, Phys. Rev. B 78 (2008) 075120.
[22] D.R. Tilley and J. Tilley, *Superfluidity and Superconductivity*, (Adam Higler, Bristol and New York, 1990); P.G. De Gennes, *Superconductivity of Metals and Alloys*, (W.A. Benjamin, Mew York, Amsterdam, 1966).
[23] M.Ya. Amusia, V.R. Shaginyan, Phys. Rev. B 63 (2001) 224507.
[24] V.A. Khodel, JETP Lett. 86 (2007) 832.
[25] M. Pfitzner, P. Wölfle, Phys. Rev. B 33 (1986) 2003.
[26] S.A. Artamonov, V.R. Shaginyan, JETP 92 (2001) 287.
[27] M.V. Zverev, Baldo, Journ. Phys. Condens. Matter 11 (1999) 2059.
[28] Yu.G. Pogorelov, V.R. Shaginyan, JETP Lett. 76 (2002) 532.
[29] D. Takahashi, et al., Phys. Rev. B 67 (2003) 180407.
[30] P. Gegenwart, et.al., Phys. Rev. Lett. 94 (2005) 076402.
[31] J. Custers, et.al., Nature 424 (2003) 524.
[32] A.P. Pikul et al., J. Phys. Condens. Matter 18 (2006) L535.
[33] J.W. Clark, V.A. Khodel, M.V. Zverev, Phys. Rev. B 71 (2005) 012401.
[34] J. Paglione et al., Phys. Rev. Lett. 91 (2003) 246405.
[35] F. Ronning, et al., Phys. Rev. B 73 (2006) 064519.
[36] P. Gegenwart, et al., Phys. Rev. Lett. 89 (2002) 056402.
[37] A. Bianchi, et al, Phys. Rev. Lett. 89 (2002) 137002.
[38] J. Paglione, et al., Phys. Rev. Lett. 97 (2006) 106606.
[39] V.R. Shaginyan, A.Z. Msezane, V.A. Stephanovich, E.V. Kirichenko, Europhys. Lett. 76 (2006) 898.
[40] V.R. Shaginyan, K.G. Popov, Phys. Lett. A 361 (2007) 406.
[41] K. Kadowaki, S.B. Woods, Solid State Comm. 58 (1986) 507. (1986).
[42] V.A. Khodel and P. Schuck, Z. Phys. B **104**, 505 (1997).